COMPUTATIONAL STUDY OF TWO-DIMENSIONAL NATURAL CONVECTION IN A CONCENTRIC HORIZONTAL ANNULUS WITH A CONSTANT HEAT FLUX WALL

Larissa Cunha Pinheiro, larissa@lasme.coppe.ufrj.br[1]
Arthur Pereira de Oliveira, arthur.pereira.oliveira@poli.ufrj.br[1]
Jian Su, sujian@lasme.coppe.ufrj.br[1]

[1]Universidade Federal do Rio de Janeiro - PEN/COPPE/UFRJ. Centro de Tecnologia - Av. Horácio Macedo, 2030 - 101 - Cidade Universitária, Rio de Janeiro - RJ, 21941-450

Abstract: *Natural convection in horizontal annulus is a fundamental heat transfer problem and can be encountered in a variety of engineering applications, such as heat exchangers, cooling of electronic components, and thermal insulation. In the present work, we studied numerically two-dimensional steady-state natural convection in a horizontal concentric annulus with the external surface at constant temperature and the inner surface at constant heat flux. The flow and heat transfer characteristics are governed by three dimensionless groups: Rayleigh number (Ra), Prandtl number (Pr), and the aspect ratio (R), defined as the ratio of external and inner radii. Computational simulations were carried out by using the CFD package ANSYS CFX 15.0. The Prandtl number is taken as 0.7. Multiple steady state solutions were found with different number of vortexes for a given aspect ratio R and Rayleigh number Ra. Flow pattern transition occurs at a critical Rayleigh number (Ra_c). The influence of the aspect ratio on heat transfer rate is determined for* $1.22 \leqslant R \leqslant 3.0$.
Keywords: *natural convection, Heat transfer, horizontal annulus, CFD*

1. INTRODUCTION

Buoyancy-driven flows in enclosures are considered as an efficient, safe and cost effective alternative of energy transport. These systems are commonly found in engineering applications ranging from decay heat removal from nuclear reactors, cooling of electronic components, aircraft fuselage insulation, dry and wet thermal storage systems to underground electrical transmissions cables (Fant *et al.*, 1991). However, the importance of natural convection induced flows are not restricted to thermal problems. Edward N. Lorenz developed the so-called Lorenz model based on meteorological observations of occurrence of deterministic, regardless chaotic, behavior originated in dynamical systems such as buoyancy driven flows (Lorenz, 1963).

In the last decades, a number of relevant works dedicated to the study of buoyant flows were published, most of them regarding Rayleigh-Bénard convection in rectangular cross section enclosures with different heating patterns, which are partially related to its analytical solutions and inherent experimental simplicity (Davis, 1968; Tavantzis *et al.*, 1978; Fusegi *et al.* e 1991 e Trias *et al.*, 2007). Due to its importance, the basic geometry consisting of concentric horizontal tubes with annulus flow, commonly a gas, is increasingly being studied but owing to the difficulty in solving the natural convection equations in an annular layer, however, only a few stability studies have been performed (Dyko *et al.* (1999)). Furthermore, the majority of these researches are focused on the problem with prescribed wall temperatures (Dirichlet boundary condition) and only a few studies applying the prescribed wall heat flux (Neumann boundary condition) can be found in literature (Hu *et al.*, 2015). Systems with the inner cylinder with a prescribed heat flux also have practical interest, such as the heat flux from electrical wire causing the heating of an external cylinder due to Joule's effect.

Despite being found in a great variety of thermal applications, natural convective flows are highly complex mathematical problems due to the nonlinearity of its governing equations, which arise from the geometrical-thermal coupled profile of the fluid field. The horizontal annulus flow is a hybrid problem and encompasses the characteristics of Rayleigh-Bénard flows at the top and, in the other hand, vertical enclosure systems at the midplane of the annulus.

In a considerable number of buoyant flows in horizontal annulus the 2D model fits properly and greatly simplify the mathematical analysis. The 2D annulus flow model are essentially determined by the Rayleigh number (Ra), Prandtl number (Pr), and the aspect ratio (R), defined as the ratio of external and inner radii. Multiple steady state solutions are found in such nonlinear phenomena which is also named the static bifurcation.

In their pioneer work, Powe *et al.* (1969) studied experimentally the flow patterns in horizontal annuli filled with air with fixed inner and outer cylinder temperatures as a function of R and Ra and identified the maximum Rayleigh number (Ra_H) bellow which the flow was steady. As a result, their work provided a flow pattern map divided into three regions according to the gap width: narrow ($R < 1.24$), moderate ($1.24 < R < 1.71$), and wide ($R > 1.71$) yielding the oscillatory, stable and multicellular 2D flow. Later, Rao *et al.* (1984) confirmed experimentally and numerically Powe's results for the narrow and moderate annulus gaps. The authors suggested that the failure in the analytical reproduction of the results for the wide gap was due to 3D effects in this region. Van De Sande and Hamer (1979) reported experimental and numerical steady and transient results from an investigation related to cooling of buried electrical cables immersed in water. The physical apparatus could provide two different R (2.31 and 5.98) and linear heating rates varying from 10 to 140 W/m.

Yoo (2003) investigated the effect of the fluid was also investigated by studying numerically natural convection between two concentric cylinders with $R = 2$ and $0.2 \leqslant Pr \leqslant 1$ with the constant surface temperature boundary condition at the outer wall and constant heat flux at inner wall. Yoo (2003) found a dual steady state solution at $Pr = 0.7$ which he called "upward" (crescent-shaped pattern) and "downward" (two counter-rotating eddies) flows, when Ra exceeded 5700. Later Yoo (2005) investigated the critical Rayleigh number (Ra_c) at which transitions occur in a concentric annulus with $R = 2$ and observed that the Ra above which dual flows exist is increased as Pr increases for the constant heat flux wall system. Petrone *et al.* (2004) analyzed the linear stability of systems with radius ratios in the range of $1.2 \leqslant R \leqslant 3$ for $Ra \leqslant 10^4$ with isothermal walls and highlighted a new stability mode that breaks the well known symmetry in basic flows and provided a Ra-R-plane bifurcation map in a attempt to foresee possible flow patterns. This map showed clearly that smalls R are extremely sensible to variations in Ra.

Hu *et al.* (2015) investigated the same system studied by Yoo (2003) ($R = 2$; $Pr = 0.7$) and found three different flow patterns at $Ra = 50,000$. The new flow mode consisting of multiple rotating eddies has a transition Ra_c of 2.4×10^4 and proved that different boundary conditions provide different flow patterns in natural convection flows. This conclusion was also reached before by Ho *et al.* (1988) during the numerical investigation of a fixed radius ratio horizontal annulus of 2.6 while analyzing different boundary conditions and thus obtaining different heat transfer rate results. This study also provided additional information upon the heat transfer mode, which happens in a pseudo-conductive way for $Ra \leqslant 10^3$ and mostly through convection for $Ra \geqslant 10^5$, and that a further increase of Pr above 7 has no apparent influence on temperature and velocities fields.

Literature comprising the wall heat flux condition providing information regarding a wide range of Ra and the transitions for several R are lacking as far as the authors are concerned. In order to fill some of these gaps in this study computational simulations are carried out applying the ANSYS CFX 15.0 package, with Pr taken as 0.7 in a range of $1.22 \leqslant R \leqslant 3$ to evaluate the different flow patterns and the Ra_c at which transitions from steady to unstable flow occur. Also the study of the heat transfer rates is performed.

2. MATHEMATICAL MODEL

We consider two dimensional, steady state, laminar natural convection in a horizontal concentric annulus as shown in Fig.1. The inner and outer radii are r_i and r_o respectively. The surface of the inner cylinder is kept at a constant heat flux q_H, while the surface of the outer cylinder is kept at a constant temperature T_0. Boussinesq approximation is adopted, i. e., considering the fluid properties constant except for the density in the buoyancy term in the momentum equations, in which is assumed to vary linearly with temperature.

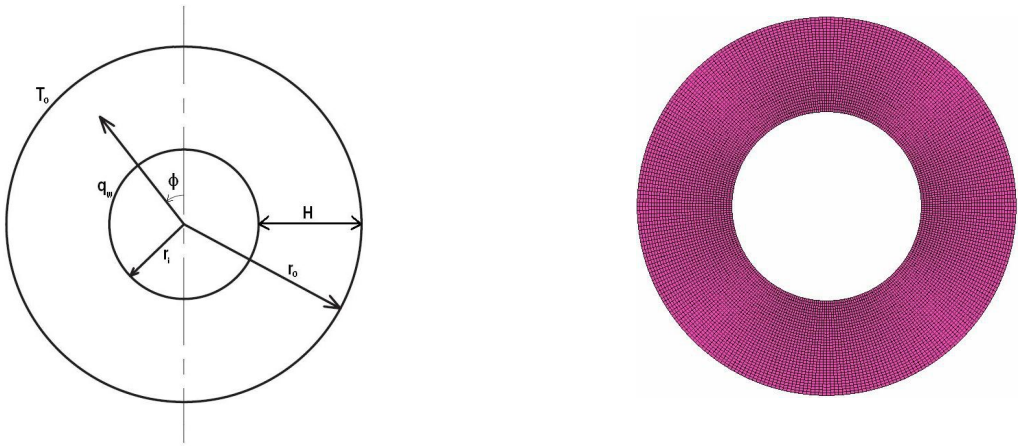

(a) **Geometry definition.** (b) **Mesh for $R = 2$.**

Figura 1: **Geometry and typical mesh.**

The dimensionless governing equations in cylindrical coordinates are written as:
Continuity equation:

$$\frac{1}{r}\frac{\partial(rv_r)}{\partial r} + \frac{1}{r}\frac{\partial v_\theta}{\partial \theta} = 0, \tag{1}$$

Momentum equation in r-direction:

$$\frac{\partial v_r}{\partial \tau} + v_r\frac{\partial v_r}{\partial r} + \frac{v_\theta}{r}\frac{\partial v_r}{\partial \theta} - \frac{v_\theta^2}{r} = -\frac{\partial p}{\partial r} + \frac{1}{r}\frac{\partial}{\partial r}\left(r\frac{\partial v_r}{\partial r}\right) + \frac{1}{r^2}\frac{\partial^2 v_r}{\partial \theta^2} - \frac{v_r}{r^2} + \frac{2}{r^2}\frac{\partial v_\theta}{\partial \theta} + \frac{Ra}{Pr}T\sin\theta, \tag{2}$$

Momentum equation in θ-direction:

$$\frac{\partial v_\theta}{\partial \tau} + v_r\frac{\partial v_\theta}{\partial r} + \frac{v_\theta}{r}\frac{\partial v_\theta}{\partial \theta} - \frac{v_r v_\theta}{r} = -\frac{1}{r}\frac{\partial p}{\partial \theta} + \frac{1}{r}\frac{\partial}{\partial r}\left(r\frac{\partial v_\theta}{\partial r}\right) + \frac{1}{r^2}\frac{\partial^2 v_\theta}{\partial \theta^2} - \frac{v_\theta}{r^2} + \frac{2}{r^2}\frac{\partial v_r}{\partial \theta} + \frac{Ra}{Pr}T\cos\theta, \tag{3}$$

Energy equation:

$$\frac{\partial T}{\partial \tau} + v_r \frac{\partial T}{\partial r} + \frac{v_\theta}{r}\frac{\partial T}{\partial \theta} = \frac{1}{Pr}\left(\frac{1}{r}\frac{\partial}{\partial r}\left(r\frac{\partial T}{\partial r}\right) + \frac{1}{r^2}\frac{\partial^2 T}{\partial \theta^2}\right) + \frac{1}{Pr}. \tag{4}$$

The dimensionless variables in Eqs. (1) - (4) are defined as follows:

$$r = \frac{r^*}{H}, \qquad v_r = \frac{v_r^*}{\nu/H}, \qquad v_\theta = \frac{v_\theta^*}{\nu/H}, \qquad \tau = \frac{t^*}{H^2/\nu} \qquad p = \frac{p^*}{\rho(\nu/H)^2}, \qquad T = \frac{T^* - T_0^*}{q_w H/k},$$

where v is the fluid velocity, T the temperautre, p the pressure, t is time, r and θ the radial and circumferential coordinates respective, ν the kinematic viscosity, ρ the fluid density, $H = r_o - r_i$ the radial gap space the outer and inner cylindrical surfaces.

Equations (1) - (4) represent a non-linear, dissipative, dynamical system. The key dimensionless parameters in these equations are the Rayleigh number Ra_H, the Prandtl number Pr, and the aspect ratio $R = r_o/r_i$. The Rayleigh number adopted in the calculation is also known as the modified Rayleigh number, since it is based on the heat flux instead of the temperature difference. These dimensionless groups are defined as:

$$Ra_H = \frac{C_p \rho \beta H^4 q_w}{k^2 \mu}, \quad Pr = \frac{\mu C_p}{k}. \tag{5}$$

Equations (1) - (4) are to be solved with the following boundary conditions:

$$v_r = v_\theta = 0, \quad \text{at} \quad r = R_i. \tag{6}$$

$$v_r = v_\theta = 0, \quad \text{at} \quad r = R_o. \tag{7}$$

$$\frac{\partial T}{\partial r} = -1, \quad \text{at} \quad r = R_i. \tag{8}$$

$$T = 0, \quad \text{at} \quad r = R_o. \tag{9}$$

where $R_i = r_i/H$ and $R_o = r_0/H$.

The ANSYS CFX package is a robust hybrid solver that uses an element-based finite volume method, which first involves discretizing the spatial domain using a mesh. The mesh is used to construct finite volumes, which are used to conserve relevant quantities such as mass, momentum, and energy (ANSYS Inc., 2013). The geometry was created in the ANSYS DesignModeler software, which is a CAD model generator specifically developed for CFD simulations. The domain discretization was generated by the ANSYS ICEM CFD software and a typical mesh for the $R = 2$ can be seen in Fig. 1b. Since CFX does not support 2D surface meshes, the geometry needs to have a relatively thin thickness in order to have just one element in the symmetry direction. This method is called the 2,5-D simulation and ensures that since it presents no other element in the non required dimension, the results will not be interpolated, yielding a 2-D only model. For each geometry a hexahedral mesh was created consisting of 20,720, 16,560, 12,800, 7,800, 8,640, 5,880 nodes for the geometries with R equals to 2, 3, 1.66, 1.4, 1.28 and 1.22, respectively. An additional geometry with $R = 2.6$ was studied and compared with literature data. A mesh convergence criteria test was performed in the $R = 3$ mesh, with a coarser and a finer mesh by a factor of 3. The relative difference of temperature between these three meshes were no greater than 0.2% and the medium mesh was taken as converged and implemented in the calculations. Also, as this is the critical case in relation to the number of nodes, the subsequent meshes were also considered as converged.

The physical model is set in the integrated software ANSYS CFX-PRE. The thermal boundary set in the inner wall is defined as constant heat flux and in the outer wall the fixed temperature of 0^oC is adopted. Once the gap width is defined as 0.01 for all geometries, the Ra_H becomes only a function of heat flux. The initial condition for all simulations, except in explicit special cases, were no angular nor radial velocity and a homogeneous temperature of 0^oC. The standard laminar viscous model was used in calculations. To complete the physical model the fluid had to be defined. The air properties at 0^oC were provided to the solver so the resulting Pr is 0.7. In steady state analysis, CFX employs the false transient algorithm with a fixed or variable timescale, which can be user defined prior to the simulation or recalculated by the solver during simulation. The former is quite safe and conservative and is adequately chosen. All simulations were done using double precision mode. Since the governing equations are nonlinear and so demanding a great number of iterations a convergence criteria of 10^{-6} is considered as the maximum residue of the conservation equations. A second convergence criteria regarding the imbalances was additionally specified as 0.001%.

3. RESULTS AND DISCUSSIONS

A number of simulations were ran to determine the transition boundary between the stable and unstable zones of the natural convection flows. A natural convection flow is considered unstable when steady state simulations did converge within the limits of 10,000 maximum iterations. Nonetheless, at the beginning of the unstable stage most of simulations would converge with greater residues, so providing information, notwithstanding more qualitative than quantitative, about the fluid and thermal field in the vicinities of the transition to the unstable zone. This information was gathered decreasing

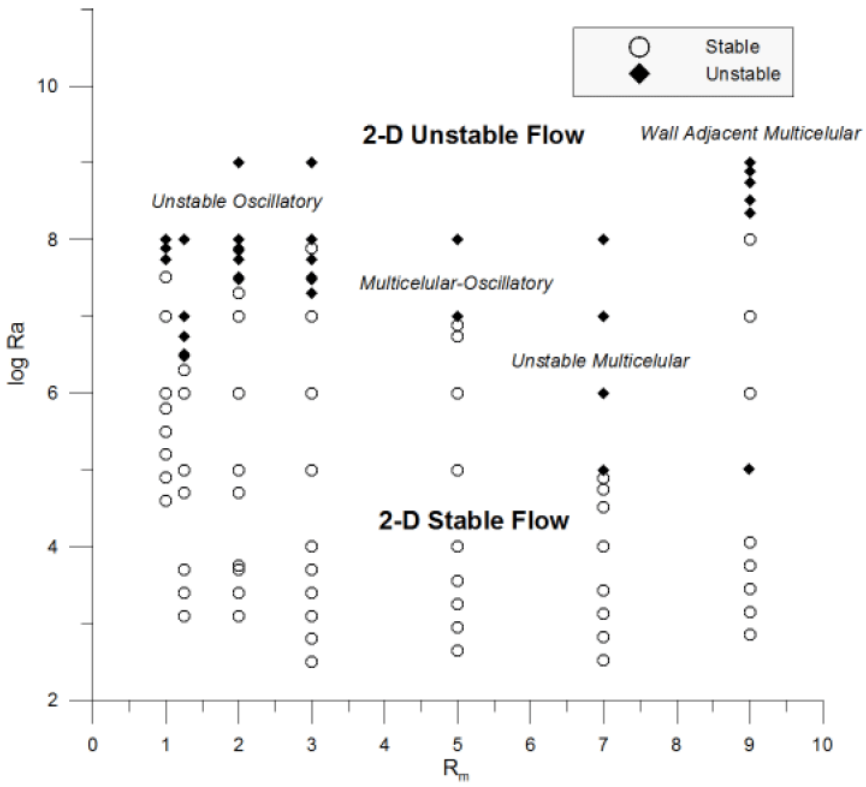

Figura 2: **Regime map of stability zones.**

the interval between the first unstable Rayleigh number and the last stable state until a satisfactory transition could be achieved. The regime map of the stability zones in Ra-R_m plane is presented in Fig.2, with $R_m = 2/(R-1)$ being the inverse gap width.

The lowest Ra obtained for $R_m = 7$ was consistent with previous results in literature. Previous work had reported this region as being soon affected by 3-D effects. Although most of the stability maps were drawn for the isothermal boundary, these studies can provide qualitative information for the heat flux boundary if Ra is the same in both cases, as pointed out by Mahfouz (2012).

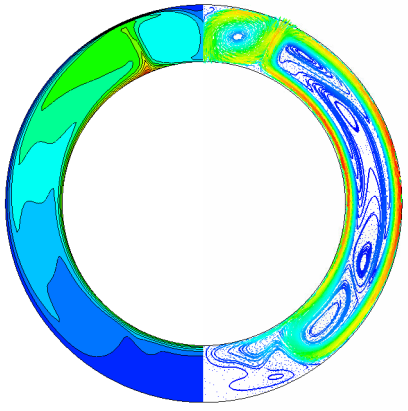

Figura 3: **New stability mode based on new condition for $R = 1.66$ and $Ra = 10^8$.**

It is also known that natural convection phenomenon has multiple steady state solutions and there exist many works dealing with the different flow patterns that arise from these solutions. It can be seen from Fig.2 that among the unstable zone for $R_m = 3$, a stable flow was obtained for $Ra = 7.75 \times 10^7$, with the same initial conditions and homogeneous heating patterns as the other surrounding flows. The convergence criteria was decreased to make sure this solution was not a numerical perturbation and the simulation managed to converge with a residue as low as 10^{-9}. Thus this simulation was used as initial guess for the other unstable points and except $Ra = 10^9$ all converged to stable solutions, showing that this zone presents the hysteresis phenomenon. The opposite behavior is found for $R_m = 9$ in $Ra_H = 10^5$ which is a unstable point in a wide stable zone is obtained. Petrone *et al.* (2004) has encountered a similar behavior for $Ra \leqslant 10^4$

and $R = 1.2$. Figure 3 shows the profile of this new solution family, which is composed by two symmetrical vortexes on the top and two long vortexes, filled with minor other vortexes, on the side.

Only the nature of the unstable zone is clarified. The oscillatory unstable flow consist in a pendulum like flow, without any axisymmetry. The oscillatory to multicelular flow is also oscillatory but multivortexes can be observed. The wall adjacent flow is basically the multicelular flow, but these vortexes are smaller and do not represent a major obstacle to the flow.

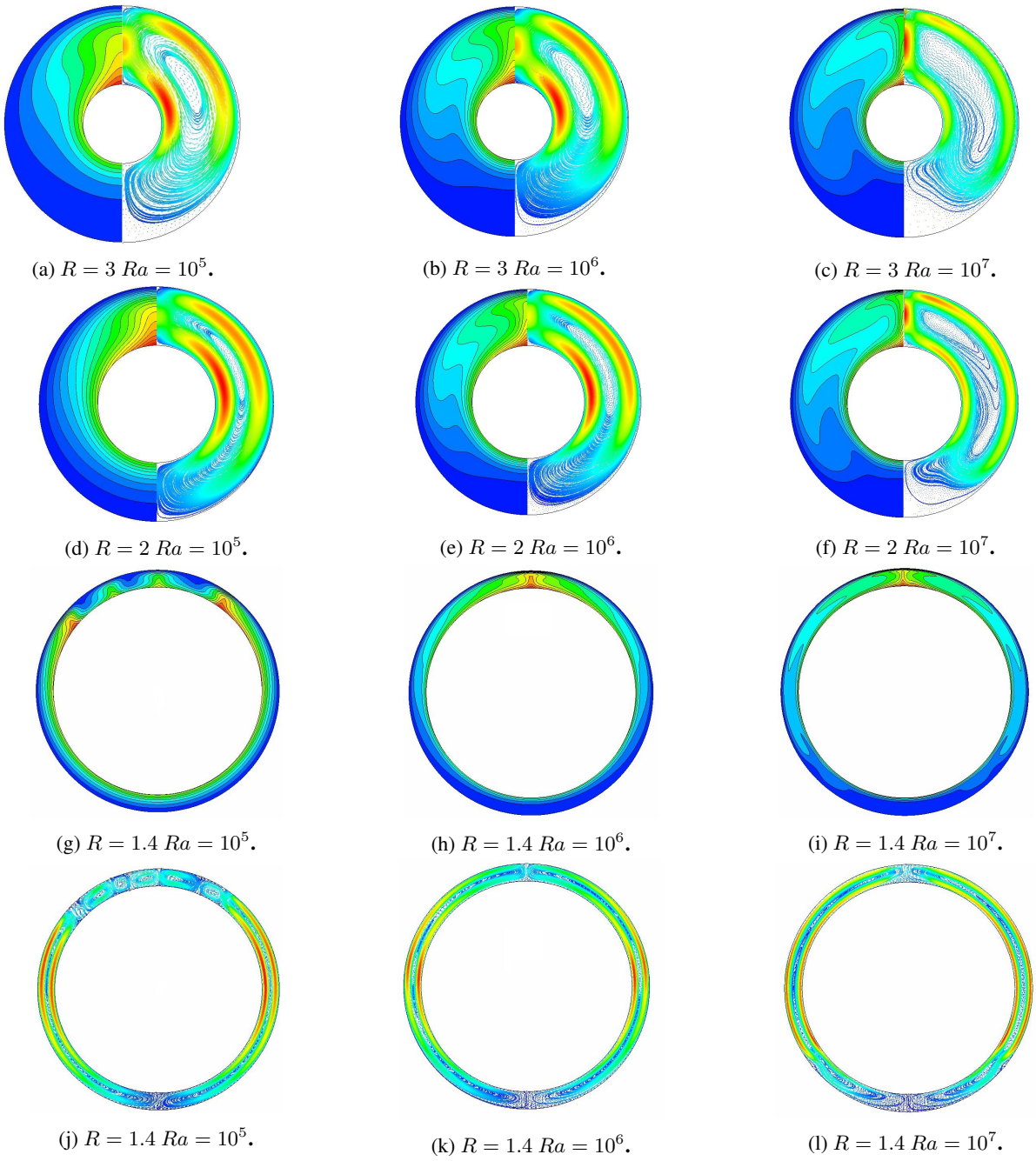

(a) $R = 3$ $Ra = 10^5$. (b) $R = 3$ $Ra = 10^6$. (c) $R = 3$ $Ra = 10^7$.

(d) $R = 2$ $Ra = 10^5$. (e) $R = 2$ $Ra = 10^6$. (f) $R = 2$ $Ra = 10^7$.

(g) $R = 1.4$ $Ra = 10^5$. (h) $R = 1.4$ $Ra = 10^6$. (i) $R = 1.4$ $Ra = 10^7$.

(j) $R = 1.4$ $Ra = 10^5$. (k) $R = 1.4$ $Ra = 10^6$. (l) $R = 1.4$ $Ra = 10^7$.

Figura 4: **From (a) - (f) isotherms on left and streamlines on right; (g) - (i) isotherms and (j) - (l) streamlines.**

Figure 4 presents isotherms and streamlines for nine combinations from three Ra and three R. For $R = 2$ and $R = 3$, the isotherms and streamlines are presented together (Fig. 4a and Fig. 4f), as the temperature and flow fields are symmetrical with respect to the middle plane. For $R = 1.4$ isotherms and streamlines are presented separately due to the asymmetrical flow found for $Ra = 10^5$. This flow pattern ais composed by five vortexes on the top and two major vortexes on the lateral and lower part of the annulus. Normally, the maximum temperature is found at the top of the annulus ($\phi = 0$). In the case showed in Fig. 4g is clearly seen that the high activity caused by the top vortexes will not allow the heat to be transported to the top of the annulus by convection. Also, no hot spots are found in this region because Ra is already sufficiently big to promote a efficient convective regime and dissipate the heat coming from the walls. That is the reason for the two regions of high temperature instead of one, nonetheless not symmetrical. Asymmetrical flows were more common in the unstable zone, since the transition occurred in a specific configuration in which thermal energy promoted a velocity profile that was unable to dissipate energy sufficiently, causing the flow to oscillate and form new

vortexes due to local enhancement in buoyancy. This behavior broke the symmetry which was sustained by the stability of the flow. However, cases of asymmetrical steady state flows like the one showed in Fig. 4g and Fig. 4j have been found in literature and strengthen the importance of the knowledge of the zone simulated, since the implementation of symmetric boundaries where there is no symmetry originates fluid fields with no physical meaning. Specifically in this case, it is most unlikely to observe the two hot spots without the full spatial model.

The average Nusselt number was used to assess the effect of the radius ratio on the heat transfer as shown Fig. 5. The average Nusselt Nu_H based on the gap width is defined by:

$$Nu_H = \frac{q_w H}{k(\overline{T}_m - T_0)}, \tag{10}$$

where $\overline{T}_m$ is the mean wall temperature at the inner cylinder.

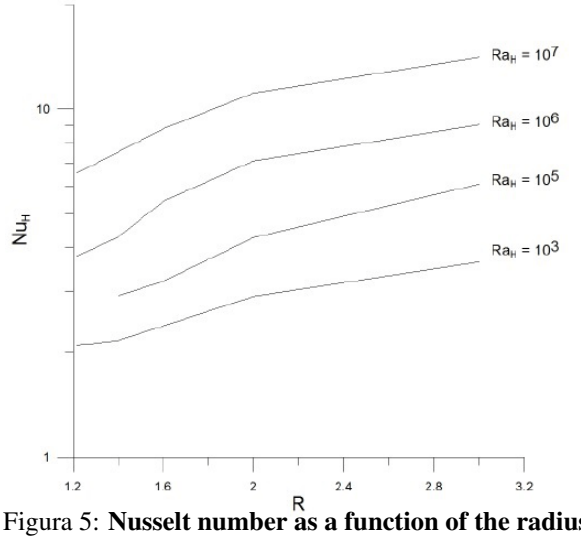

Figura 5: **Nusselt number as a function of the radius ratio.**

The aspect ratio has a nonlinear influence on the heat transfer and hence a constant exponent regarding the influence of R should not be used. It is also observed in Fig. 5 a major inclination at the beginning, when leaving the conduction zone, and a tendency to converge for certain value of Nu_H in all curves. This behavior is expected and as predicted by Kumar (1988) the system will achieved the same thermal characteristics of the single cylinder in R beyond 15. One could also conclude that the reason for this convergence value of Nu_H bigger for the free cylinder is because the introduction of the inner cylinder enhance the friction force and the presence of the wall as a flow restriction also increase the probability of low effective heat transfer zones as in the center of vortexes.

For all aspect ratios, increasing of heat flux also increases the heat transfer profile after the conduction regime (Fig.6). At high R geometries this effect is less pronounced. This fact results from the larger relatively resistance faced by the fluid in high R, provided the same gap width. Worth noting that even if the rate of heat transfer is slower for the high diameter ratio cases, the heat transfer itself is bigger due to the effects already listed.

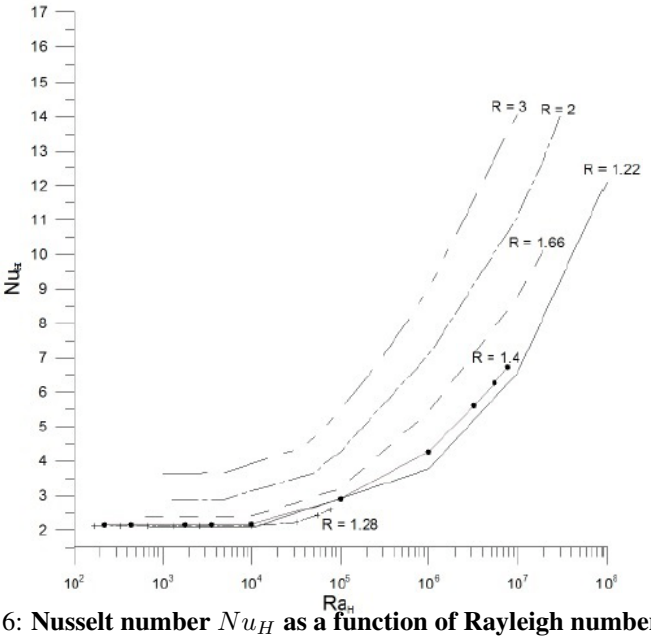

Figura 6: **Nusselt number Nu_H as a function of Rayleigh number Ra_H**

Finally, a comparison between the average Nusselt number for isothermal boundary and wall heat flux boundary conditions is performed. In order to fairly compare both heat transfer results the system has to be under similar conditions of Ra and R, and additionally the following necessary condition has to be respected:

$$T_i - T_o = \overline{T}_m - T_o, \tag{11}$$

where $(T_i - T_o)$ is the applied temperature difference in the case of isothermal boundaries. The Rayleigh number based on temperature difference (Ra^*) can be derived from the above condition providing:

$$Ra^* = \frac{Ra_H}{Nu_H}. \tag{12}$$

Projahn and Beer (1985) realized an experimental study with isothermal walls in eccentric e concentric annuli with $R = 2.6$. They used data regression to yield a correlation with validity in the range of $0.7 \leqslant Pr \leqslant 7.0$, and $Ra^* \geqslant 7\times10^3$ with a relative error within 3%, presented for concentric annulus in Eq. 13.

$$\Gamma = 0.212 Ra^{*0.243}, \quad \Gamma \equiv \frac{Nu_{r_i}}{N_c}, \tag{13}$$

where Γ is the equivalent conductivity, Nu_{r_i} is the average Nusselt number based on the inner radius and Nu_c is the Nusselt in the conduction regime.

With the appropriate modifications, the correlation can be rewritten in terms of Ra_H in the form:

$$Nu_H = 0.4347 Ra_H^{0.1955}, \quad Ra_H > 21364. \tag{14}$$

In all the range of Fig.7 the system with a prescribed heat flux yielded higher heat transfer rates than the system under the same conditions applying the isothermal walls. Similar results were predicted by Kumar (1988). This trend arises from the much bigger temperature gradient developed in the case of wall heat flux boundary.

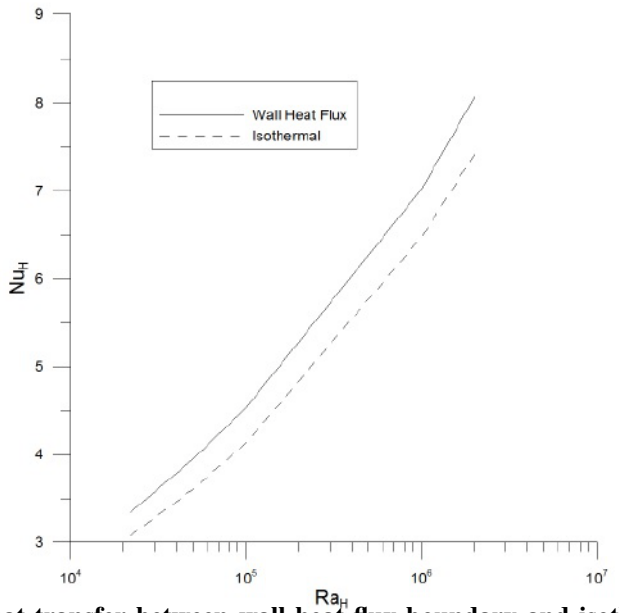

Figura 7: **Comparison of heat transfer between wall heat flux boundary and isothermal boundary obtained by Projahn and Beer (1985).**

4. CONCLUSION

A CFD study applying the ANSYS CFX 15.0 package was realized and has provided information regarding the stability zones found in natural convective flows in horizontal concentric annulus. Within well delimited areas of stability/instability non conformal points were found, evidencing the presence of hysteresis for the $R = 1.66$ in Ra_H near 7×10^7 and $R = 1.22$ for $Ra_H \approx 10^5$. The stable mode within the unstable zone was studied and its profiled was showed. Also, an asymmetrical stable mode consisting of 7 vortexes was presented, emphasizing the need of full spatial simulation in order to find multiple steady-state solutions and accurate calculations on the maximum temperatures and velocities. These parameters are important in the design of the annulus systems so that surface overheating can be avoided.

The aspect ratio was found to have a nonlinear effect on the heat transfer, measured by the average Nusselt number. This influence, however, is small and as the R increases the tendency is to converge for the free cylinder thermal behavior. Finally, a comparison between the wall heat flux boundary and the isothermal boundary was performed providing better results for the wall heat flux boundary.

For future works, a study of the zone which was classified as being subjected to hysteresis should be investigated. Also, more information on the mechanisms of the unstable flows are needed.

5. ACKNOWLEDGEMENTS

The authors thank gratefully CNPq and FAPERJ for providing the financial support for this study. Larissa C. Pinheiro thanks CNEN for a MSc scholarship.

6. REFERENCES

ANSYS Inc., 2013. "ANSYS CFX-Solver Theory Guide".

Davis, G.d.V., 1968. "LAMINAR NATURAL CONVECTION IN A ENCLOSED RECTANGULAR CAVITY". *Journal of Heat and Mass Transfer*, Vol. 11, pp. 1675–1693.

Dyko, M.P., Vafai, K. and Mojtabi, A.K., 1999. "A numerical and experimental investigation of stability of natural convective flows within a horizontal annulus". *Journal of Fluid Mechanics*, Vol. 381, pp. 27–61.

Fant, D.B., Rothmayerf, A. and Prusat, J., 1991. "Natural Convective Flow Instability Between Horizontal Concentric Cylinders". *Journal of Thermophysics*, Vol. 5, No. 3, pp. 407–415.

Fusegi, T., Hyun, J.M., Kuwaharas, K. and Farouk, B., 1991. "A numerical study of three-dimensional natural convection in a differentially heated cubical enclosure". *Journal of Heat and Mass Transfer*, Vol. 34, No. 6, pp. 1543–1557.

Ho, C.J., Lin, Y.H. and Chen, T.C., 1988. "A numerical study of natural convection in concentric and eccentric horizontal cylindrical annuli with mixed boundary conditions". *International Journal of Heat and Fluid Flow*, Vol. 10, No. 1, pp. 40–47.

Hu, Y., Li, D., Shu, S. and Niu, X., 2015. "Transfer Study of multiple steady solutions for the 2D natural convection in a concentric horizontal annulus with a constant heat flux wall using immersed boundary-lattice Boltzmann method". *International Journal of Heat and Mass Transfer*, Vol. 81, pp. 591–601.

Kumar, R., 1988. "Study of natural convection in horizontal annuli". *International Journal of Heat and Mass Transfer*, Vol. 31, No. 6, pp. 1137–1148.

Lorenz, E.N., 1963. "Lorenz 1963 - Deterministic non periodic flow.pdf". *Journal of the Atmospheric Sciences*, Vol. 20, pp. 130–141.

Mahfouz, F.M., 2012. "Heat Convection Within an Eccentric Annulus Heated at Either Constant Wall Temperature or Constant Heat Flux". *Journal of Heat Transfer*, Vol. 134, No. August, p. 082502.

Petrone, G., Ch, E. and Lauriat, G., 2004. "Stability of free convection in air-filled horizontal annuli : influence of the radius ratio". *Journal of Heat Transfer and Mass Transfer*, Vol. 47, pp. 3889–3907.

Powe, R.E., Carley, C.T. and Bishop, E.H., 1969. "Free convective flow patterns in cylindrical annuli". *ASME Journal of Heat Transfer*, Vol. 91, No. 310 - 314.

Projahn, U. and Beer, H., 1985. "Prandtl number effects on natural-convection heat-transfer in concentric and eccentric horizontal cylindrical annuli". *Warme Und Stoffubertragung-Thermo and Fluid Dynamics*, Vol. 19, No. 4, pp. 249–254.

Rao, Y.F., Miki, Y., Fukuda, K., Takata, Y. and Hasegawa, S., 1984. "Flow patterns of natural convection in horizontal cylindrical annuli". *International Journal of Heat and Mass Transfer*, Vol. 28, No. 3, pp. 705–714.

Tavantzis, J., Reiss, E.L. and Matkowsky, B.J., 1978. "On the Smooth Transition to Convection". *SIAM Jorunal of Applied Mathematics*, Vol. 34, No. 2, pp. 322–337.

Trias, F.X., Soria, M., Oliva, A. and Pérez-Segarra, C.D., 2007. "Direct numerical simulations of two- and three-dimensional turbulent natural convection flows in a differentially heated cavity of aspect ratio 4". *Journal of Fluid Mechanics*, Vol. 586, pp. 259–293.

Van De Sande, E. and Hamer, B.J.G., 1979. "Steady and transient natural convection in enclosures between horizontal circular cylinders (constant heat flux)". *International Journal of Heat and Mass Transfer*, Vol. 22, No. 3, pp. 361–370.

Yoo, J.S., 2003. "Dual free-convective flows in a horizontal annulus with a constant heat flux wall". *International Journal of Heat and Mass Transfer*, Vol. 46, No. 2003, pp. 2499–2503.

Yoo, J.S., 2005. "Flow pattern transition of natural convection in a horizontal annulus with constant heat flux on the inner wall". *International Journal of Numerical Methods for Heat {&} Fluid Flow*, Vol. 15, No. 7, pp. 698–709.

7. RESPONSIBILITY NOTICE

The authors are the only responsibles for the printed material included in this paper.